Collective electromagnetic excitations in a double-layer two-dimensional electron system in a high magnetic field

I. E. Aronov
Theoretical Division and the CNLS, Los Alamos National Laboratory, Los Alamos, New Mexico 87545
and Institute for Radiophysics and Electronics, National Academy of Sciences of Ukraine, 12 Acad. Proskura St., Kharkov 310085, Ukraine

N. N. Beletskii
Institute for Radiophysics and Electronics, National Academy of Sciences of Ukraine, 12 Acad. Proskura St., Kharkov 310085, Ukraine

G. P. Berman and A. R. Bishop
Theoretical Division and the CNLS, Los Alamos National Laboratory, Los Alamos, New Mexico 87545
(Received 28 January 1997)

A new type of collective electromagnetic excitations, namely the surface polaritons (SP's), in a double-layer two-dimensional electron system (DL2DES) (of nn-type, pp-type, and np-type) in a high magnetic field is predicted. Using a Wigner distribution function formalism, we investigate the spectrum, damping, and polarization of the SP's in a wide range of the frequencies ω and the wave vectors $\mathbf{k}$. It is shown that near the cyclotron resonance (CR) ($\omega \sim \Omega = eB/mc$) the phase velocity of the SP's is drastically slowed down, and the group velocity undergoes the fundamental steps defined by the fine-structure constant $\alpha = e^2/\hbar c$ (as well as for the one-layer 2DES). For the nn-type DL2DES, each dispersion curve splits, and strongly correlated collective electromagnetic excitations propagate in the system. The group velocity of these excitations is defined by the interlayer distance d, and is much smaller than that for the one-layer 2DES. In the vicinity of a CR subharmonic ($\omega \sim 2\Omega$) the negative (anomalous) dispersion of the SP occurs. For the np-type DL2DES the branches of the dispersion curves are intercrossed in the long-wave region, near the subharmonic (hole) CR, and in the short-wave region, due to the resonance interaction between the principal (electron) CR mode and the subharmonic (hole) CR mode. The relaxation of the electrons (or holes) in the DL2DES leads to the occurrence of a dissipative collective mode of the SP type—the ''additional SP's'' (ASP's). This mode exists under certain threshold condition, which is determined by a fine-structure constant α. As a consequence, the dispersion curves for these excitations exhibit spectrum endpoints, and mode's confluence. The threshold condition for the ASP's in the DL2DES has a ''geometrical oscillating'' form due to the coherence effects between the split ASP modes. The potential importance for various applications in microelectronics is discussed. [S0163-1829(97)08339-2]

I. INTRODUCTION

Recent technological progress has made it possible to produce double-layer two-dimensional (2D) electron-gas systems (DL2DES's) of extremely high mobility.[1,2] As is illustrated schematically in Fig. 1, these systems consist of a pair of 2D electron gases (2DEG) separated by a distance d. Many authors[1–9] have discussed very interesting strong correlations effects between the layers in a high magnetic field which were predicted to lead to fractional quantum Hall effects (FQHE's). When the layer separation d is sufficiently small and comparable to the typical separation of electrons within a layer, the correlations in the strong magnetic field are especially important because all electrons can be accommodated within the lowest Landau level, and execute their cyclotron orbits with the same kinetic energy. The FQHE occurs when the system has a gap for ''induced charged excitations.'' The theory[10] predicts that at some Landau-level filling factor (even for the system of noninteracting 2DEG inside a layer) this gap in the double-layer system may occur only if the interlayer interaction is sufficiently strong. In Ref. 11 the topological excitations in the double-layer quantum Hall systems were investigated. In Ref. 12 the integer quantum Hall effect (IQHE) for nonintracting double-layer electron systems was investigated in the presence of disorder. Experimental studies[13,14] have been devoted to the investigation of the double-layer electron systems in a high magnetic field, and have observed the many-body interactions of electrons in coupled quantum double wells,[13] and the tunneling between parallel two-dimensional electron gases.[14]

In this paper we consider a DL2DES (see Fig. 1) when the interlayer length d is large enough that tunneling between the two layers is negligible. Therefore we do not consider the effects of interlayer coherence, which could be important when the tunneling between the layers is considerable.[3,4] We demonstrate that in this system a different type of collective electromagnetic excitations [viz., slow surface polaritons (SP's)] exist. These types of collective electromagnetic excitations produce strongly correlated electromagnetic modes, whose velocity are relatively small.

Surface polaritons are electromagnetic waves that propagate along a flat surface which separates two dielectric media, and whose amplitudes decay exponentially with increasing distance from the surface into either medium. In recent

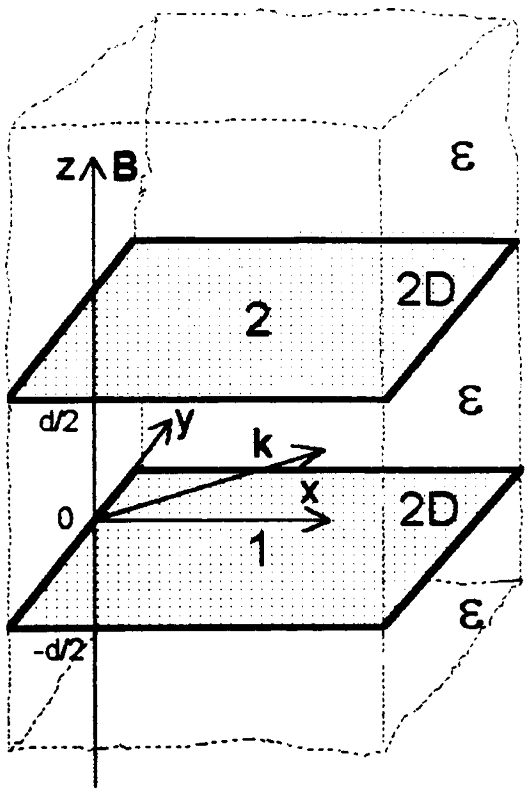

FIG. 1. The geometry of the structure of a double-layer two-dimensional electron-gas system DL2DES embedded in a dielectric medium with the dielectric constant, ε; d is the distance between two layers.

years considerable interest arose in the study of the SP in a 2DES (Ref. 15) and superlattices (see, e.g., Ref. 16). In Ref. 17 the magnetoplasma oscillations in a 2DES in a magnetic field were investigated. In Ref. 18 the magnetoplasmon excitations in a double-quantum-well system were investigated. The authors of Ref. 18 calculated the collective plasma excitations in a high magnetic field when only the lowest Landau level is occupied at zero temperature. They calculated the magnetoplasmon's spectrum in the semiclassical limit.

Many authors have investigated the weak damping of collective electromagnetic waves in 2DES in a high magnetic field.[19,21,22] The quantization of the Hall conductivity, vanishingly small dissipative (longitudinal) conductivity, and spatial and temporal dispersion of the conductivity tensor lead to the generation of an unusual collective wave, whose dispersion characteristics are also quantized.[22] It was shown in Ref. 22 that near the cyclotron resonance (CR) ($\omega \sim \Omega$) the phase velocity of the SP for the one-layer 2DES is drastically slowed down, and their group velocity undergoes fundamental jumps, whose magnitude is determined by the fine-structure constant $\alpha = e^2/\hbar c$. The number of the slow SP modes is specified by the magnitude of the Landau-level filling factor $\mathfrak{N} = \pi l^2 n$ [where $l = (c\hbar/eB)^{1/2}$ is the magnetic length, n is the density of 2D electrons, and B is the magnetic field in the 2DES], i.e., by the value of the quantized Hall conductivity. In the vicinity of the CR subharmonic ($\omega \sim 2\Omega$), the negative (anomalous) dispersion of SP's (see Fig. 3) occurs. Also, a different type of SP's of a dissipative nature (namely, ''additional surface polaritons''—ASP's) appear near the CR. The condition for the existence of these ASP's is determined by the quantized threshold criterion, which allows one to determine the relaxation frequency at low temperature to an accuracy of α.

In this paper a new type of collective electromagnetic excitations (viz., the slow SP's) in a DL2DES in a high magnetic field is predicted. We have investigated the spectrum, damping, and polarization of the SP in a wide range of frequencies ω and wave vectors $\mathbf{k}$. Various types of the DL2DES, namely nn-, pp-, and np-types of layers are considered. It is shown that near each CR [electron CR (n-type) and hole CR (p-type)] the phase velocity of the SP is drastically slowed down, and their group velocity undergoes the fundamental steps determined by the fine-structure constant α. In the DL2DES each dispersion curve splits into the two modes—one is slower than in the one-layer system, and the other one is faster. The splitting width is determined by the values of Landau-level filling factors in the layers and by the separation distance d between the layers (nn-type DL2DES). For the pn-type DL2DES strong interacting modes are excited. In the long-wave regime these interacting modes exist near the subharmonic of the holes CR. In the short-wave regime there are interacting modes between the SP of the hole layer (subharmonic of the hole CR) and the SP of the electron layer (principal electron CR). The relaxation of the conduction electrons in each layer gives rise to dissipative threshold-type modes of the ASP for the DL2DES.

The paper is organized as follows. In Sec. II we use the formalism of the Wigner distribution function (WDF) for describing the quantum transport phenomena in a 2DES in a high magnetic field (under the IQHE conditions). In Sec. III the electrodynamics in the DL2DES in a high magnetic field is presented. In this section we derive the dispersion relation for electromagnetic surface waves and discuss the dispersion, polarization, and damping for the SP in this system. In Sec. III we consider the DL2DES of nn, pp, and np types. Section IV concludes the paper with a brief summary of results and possible applications.

II. TRANSPORT IN A 2DES IN A HIGH MAGNETIC FIELD

To find a conductivity tensor that accounts for the spatial and temporal dispersion in a 2D electron gas placed in a high magnetic field $\mathbf{B}$ oriented normally to the 2D layer (see Fig. 1), we apply the WDF formalism:[22–25]

$$f^W_{\mathbf{p}}(\mathbf{r},t) = \int d\mathbf{r}' \ \mathrm{Tr}\left\{ \hat{\rho} \ \exp\left[-i\left(\mathbf{p} + \frac{e}{c}\,\mathbf{A}(\mathbf{r},t) \right)\mathbf{r}' \right] \times \psi^\dagger(\mathbf{r}-\mathbf{r}'/2)\,\psi(\mathbf{r}+\mathbf{r}'/2) \right\}. \tag{2.1}$$

Here $\hat{\rho}$ is the density matrix operator of the system; $\psi^\dagger(\mathbf{r})$ and $\psi(\mathbf{r})$ are the Fermi operators of creation and annihilation of a particle at the point $\mathbf{r}$, respectively; $\mathbf{A}$ is the vector potential of the electromagnetic field. (The effectiveness of the WDF approach to the modeling of mesoscopic solid-state devices was demonstrated in Refs. 26, 27.) In the case when the scale of the spatial inhomogeneity exceeds both the radius of interaction between the particles and the de Broglie electron wavelength, the kinetic equation for the WDF (2.1) takes the form[22–25] equivalent to the classical kinetic equation:

$$\frac{\partial f_{\mathbf{p}}^{W}}{\partial t}+\mathbf{v}\,\frac{\partial f_{\mathbf{p}}^{W}}{\partial \mathbf{r}}+e\left\{\mathbf{E}+\frac{1}{c}\,[\mathbf{v},\mathbf{B}]\right\}\,\frac{\partial f_{\mathbf{p}}^{W}}{\partial \mathbf{p}}=\hat{I}\{f_{\mathbf{p}}^{W}\}. \tag{2.2}$$

Here **E** and **B** are the electric field and the magnetic induction vectors; e is the electron charge, and **v** is the velocity of the conduction electrons.

In the case under consideration, the 2D electron system is extended in the xy plane (see Fig. 1), and the typical scale of the field's inhomogeneity is the wavelength k^{-1} of the collective electromagnetic wave. Thus, the conditions for applicability of Eq. (2.2) are $k \ll n^{1/2}$ (since at weak screening the value of $n^{-1/2}$ is the characteristic length of the interaction between particles), and $kl \ll 1$ [since the magnetic length $l=(c\hbar/eB)^{1/2}$ represents the de Broglie wavelength of electrons in a high magnetic field]. The collision integral, $\hat{I}\{f_{\mathbf{p}}^{W}\}$, in Eq. (2.2) differs essentially from the classical collision integral, since the quantum transitions contributing to $\hat{I}\{f_{\mathbf{p}}^{W}\}$ reflect the character of the particle's statistics, and a distinction of the WDF from the classical one.[24] The equilibrium WDF sets the collision integral $\hat{I}\{f_{\mathbf{p}}^{W}\}$, to zero. The equilibrium WDF can be expressed via its value for an equilibrium ensemble of quantum states of an electron in a magnetic field **B**. Using the definition (2.1), and substituting the wave functions of an electron in an electromagnetic field into Eq. (2.1), we obtain the equilibrium WDF for spinless electrons,[22,24,25]

$$f_0(\epsilon)=\sum_{s=0}^{\infty} n_F\left[\frac{\hbar\Omega(s+\frac{1}{2})-\mu}{T}\right]\Gamma_s\left(\frac{\epsilon}{\hbar\Omega}\right),$$

$$\Gamma_s(x)=2(-1)^s\,\exp(-2x)L_s^{(0)}(4x),$$

$$n_F(x)=(1+e^x)^{-1}. \tag{2.3}$$

Here $\epsilon=p^2/2m$ is the energy of 2D electrons, μ is the chemical potential, T is the temperature, and $L_s^{(0)}(x)$ is the Laguerre polynomial. If we replace the summation over s in Eq. (2.3) by integration, then for $\hbar\Omega \ll T$, Eq. (2.3) transforms into an equilibrium Fermi distribution function.

Using the equilibrium WDF (2.3), we can derive all thermodynamical relations. In this paper we will consider the 2DES when the chemical potential μ is constant over the entire 3D system (i.e., the grand canonical electron system).

Figures 2(a)–2(f) demonstrate the equilibrium WDF (2.3) as a function of ϵ/μ at $T=50$ mK, $\mu=20$ meV, and for different values of the magnetic field B (and, correspondingly, for the different values of the Landau-level filling factor, $\mathfrak{N}=\pi l^2 n$). It is easy to see that at high magnetic field, $\hbar\Omega \gg T$, [Fig. 2(a)] the edge of the Fermi distribution function in the electron distribution does not manifest itself, and the WDF (2.3) decays exponentially, $\sim\exp(-2\epsilon/\hbar\Omega)$. Figure 2(b) displays the equilibrium WDF for $\mathfrak{N}=3$. In this case the equilibrium WDF has one minimum and one maximum as a function of energy ϵ. When $\mathfrak{N}$ increases [see Figs. 2(c), 2(d), 2(e), 2(f)] the equilibrium WDF (2.3) oscillates as a function of energy, and transforms to the Fermi distribution function, when the magnetic field diminishes. Thus, the WDF formalism takes into account quantization of the electron spectrum in a magnetic field as intrinsic properties, and makes it possible to describe the electron transport and equilibrium properties in terms of classical variables. In this way, the description of the quantum kinetics becomes highly transparent.

The relation between the electron density n and the chemical potential μ in a high magnetic field can be found, as usual, from the normalization condition. Below we will consider the 2DES with a fixed value of the chemical potential μ. The real 2DES is in fact extremely inhomogeneous in one of the directions of a 3D electron system. A 2DES occurs, for example, in the inversion layers of a metal-oxide-semiconductor-field-effect transistor, or in the $GaAs-Al_xGa_{1-x}As$ heterostructures at low temperature. In such systems the chemical potential μ is determined for the 2DES as an equilibrium value of μ for an extremely inhomogeneous 3D systems. The density n of the 2D electrons is an average of $f_0(\epsilon)$ Eq. (2.3). As a result, we obtain after averaging the expression for the Landau-level filling factor,

$$\mathfrak{N}=\pi l^2 n=\sum_{s=0}^{\infty} n_F\left[\frac{\hbar\Omega(s+\frac{1}{2})-\mu}{T}\right]. \tag{2.4}$$

Below we assume that the IQHE conditions are satisfied: $\hbar\Omega/T \gg 1$, $\mu/T \gg 1$.

The formalism used in this paper is based on the assumption that the kinetic equation for the WDF (2.2) can also involve the collision integral. Usually, the kinetic approach based on the collision integral can be justified under the condition $k_F l^* \gg 1$, where k_F is the Fermi wave number of an electron, and l^* is the characteristic electron's mean free path.[28–33] We will consider in this paper the effects determined by the linear response to the electric field. In this case the WDF, $f_{\mathbf{p}}^{W}$, can be found in a linear approximation with respect to the external field, **E**. It is well known[24] that for a sample with a high electron mobility and in the high-frequency regime ($\omega\tau \gg 1$) the collision integral can be used in the τ approximation, where the mean-free-path time τ is determined by the relaxation frequency $\nu(\epsilon)=\tau^{-1}$, a function of the electron energy, ϵ.

In the following we assume that the distance d between the two layers is large enough, and the potential barrier between the layers is rather high. In this case, tunneling and strong electron correlation effects can be neglected, and we can consider the electron's kinetics in both layers independently. We represent the WDF in each layer in the form

$$f_{\mathbf{p}}^{W}=f_0(\epsilon)+f_1, \tag{2.5}$$

where $f_0(\epsilon)$ and $f_1 \equiv f_1(\mathbf{p},\mathbf{r},t)$ are the equilibrium and nonequilibrium parts of the WDF, respectively. In the τ approximation the collision integral, $\hat{I}\{f_{\mathbf{p}}^{W}\}$, can be written as

$$\hat{I}\{f_{\mathbf{p}}^{W}\}=-\nu(\epsilon)f_1. \tag{2.6}$$

Generally, the electric field **E** in Eq. (2.2) is a function of three coordinates and time. Then for the Fourier transforms of the current density, **j**, and the electric field, **E**, one obtains the following linear relations:

$$j_\alpha(\omega,\mathbf{k})=\sigma_{\alpha\beta}(\omega,\mathbf{k})\mathcal{E}_\beta(\omega,\mathbf{k}) \quad (\alpha,\beta=x,y), \tag{2.7}$$

where

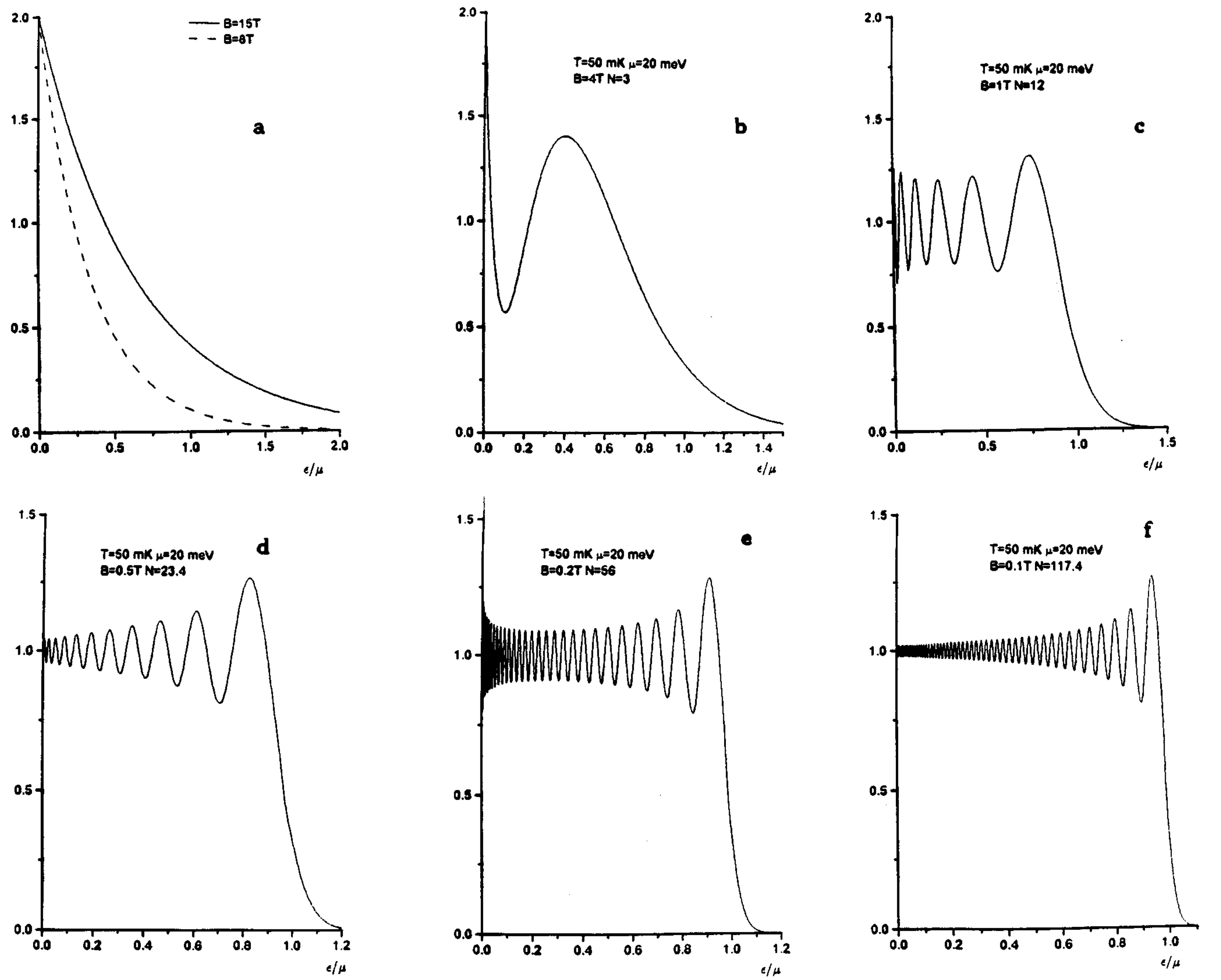

FIG. 2. The equilibrium Wigner distribution function of electrons in a magnetic field. Each figure (a)–(f) shows the value of the magnetic field B, and the Landau-level filling factor N. The value of the chemical potential is chosen as $\mu = 20$ meV.

$$E_\alpha(\mathbf{r},t)=\int \frac{d^2k\ d\omega}{(2\pi)^3}\ \mathcal{E}_\alpha(\omega,\mathbf{k})e^{i(\mathbf{kr}-\omega t)}, \tag{2.8}$$

$$\mathcal{E}_\alpha(\omega,\mathbf{k})=\int d^2k\ d\omega\ E_\alpha(\omega,\mathbf{k})e^{i(\mathbf{kr}-\omega t)}. \tag{2.9}$$

The Fourier transform of the conductivity tensor, $\sigma_{\alpha\beta}(\omega,\mathbf{k})$ can be found from Eqs. (2.2)–(2.6). In the general case we have, for the conductivity tensor in each layer, the same equation as the one derived in Ref. 22.

In this paper we will assume that the mobility of electrons is very high, and the relaxation frequency is an effective constant, i.e., $\nu=$const. We will consider the most realistic case, when the spatial dispersion is sufficiently weak, i.e,

$$kl \leqslant 1. \tag{2.10}$$

Then the Fourier transform of the conductivity tensor in each layer can be represented in the form

$$\sigma_{\alpha\beta}=\frac{2e^2}{h}\frac{\mathfrak{N}}{1+\gamma^2}\left\{B_{\alpha\beta}-\frac{(kl)^2}{2\gamma}\left(1+\frac{\mathfrak{N}}{2}\right)C_{\alpha\beta}\right\}, \tag{2.11}$$

where

$$B_{xx}=B_{yy}=\gamma,\quad B_{xy}=-B_{yx}=1,$$

$$C_{xx}=a+\cos 2\beta,\quad C_{yy}=a-\cos 2\beta,$$

$$C_{xy}=-b-\sin 2\beta,\quad C_{yx}=b-\sin 2\beta.$$

$$a=\frac{2(\gamma^2+2)}{\gamma^2+4},\quad b=\frac{6\gamma}{\gamma^2+4}. \tag{2.12}$$

From Eq. (2.14) we derive the formulas for the resistance tensor in the dc case, when $\omega\to 0$, $k\to 0$ (IQHE),

$$\rho_{xx}=\frac{\sigma_{xx}}{\sigma_{xx}^2+\sigma_{xy}^2}=\frac{h}{2e^2}\frac{\gamma}{\mathfrak{N}}, \tag{2.13}$$

$$\rho_{xy}=\frac{\sigma_{xy}}{\sigma_{xx}^2+\sigma_{xy}^2}=\frac{h}{2e^2}\frac{1}{\mathfrak{N}}. \tag{2.14}$$

As one can see, Eqs. (2.13) and (2.14) are rather convenient for describing the IQHE (see also Ref. 34), even at $\nu=$const. Equation (2.11) and Eq. (2.13) show that, if

$\nu=$const, then the relation $\rho_{xx}/\rho_{xy}=\gamma=\nu/\Omega$ should exist, which can be observed under the IQHE condition. The deviation from this simple relation demonstrates the energy dependence of the relaxation frequency, $\nu=\nu(\epsilon)$ (see Ref. 34). Equation (2.14) describes the line shape of t the CR (the high-frequency absorption is proportional to Reσ_{xx}) for various frequencies, ω, as a function of the magnetic field. Obviously, the line shape of the CR is highly sensitive to its position. In the case when the center of the resonant line is located at the center of the IQHE plateau, it shows kink-type behavior at the points where the jumps of the IQHE occur.[22] It is easy to see from Eq. (2.14) (see, also, Ref. 22) that the resonant line, whose center is located at the centre of the IQHE plateau, has structures on the wings of the resonant line at the values of magnetic field **B** corresponding to the jumps of the Landau-level filling factor $\mathfrak{N}$. The amplitude of a CR resonant line increases when the center of the CR line is located at the point of a jump of the Landau-level filling factor $\mathfrak{N}$. Such features of the CR resonant line were observed by a number of authors.[34,35]

III. ELECTRODYNAMICS OF DOUBLE-LAYER 2DES IN A HIGH MAGNETIC FIELD

The propagation of the electromagnetic waves in the systems with a 2D electron gas placed in a dielectric environment, in a strong magnetic field (see Fig. 1), is described by the Maxwell equations for the scalar and vector potentials, i.e., in the Lorentz gauge,

$$\nabla\mathbf{A}+\frac{\varepsilon}{c}\frac{\partial\varphi}{\partial t}=0. \tag{3.1}$$

The potentials **A** and φ satisfy the usual wave equation,[36,37]

$$\left[\nabla^2-\frac{\varepsilon}{c^2}\left(\frac{\partial}{\partial t}\right)^2\right]\varphi(\mathbf{r},t)=-\frac{4\pi}{\varepsilon}\rho_{\rm tot}(\mathbf{r},t), \tag{3.2}$$

$$\left[\nabla^2-\frac{\varepsilon}{c^2}\left(\frac{\partial}{\partial t}\right)^2\right]\mathbf{A}(\mathbf{r},t)=-\frac{4\pi}{c}\mathbf{j}_{\rm tot}(\mathbf{r},t). \tag{3.3}$$

These values are related to the fields in Eq. (2.2) as

$$\mathbf{E}=-\nabla\varphi-\frac{1}{c}\frac{\partial\mathbf{A}}{\partial t},\quad \mathbf{B}={\rm rot}\mathbf{A}. \tag{3.4}$$

Here $\rho_{\rm tot}=\rho_{\rm ex}+\rho$ is the total charge density in the system, and $\mathbf{j}_{\rm tot}=\mathbf{j}_{\rm ex}+\mathbf{j}$ is the total current density; $\rho_{\rm ex}$ and $\mathbf{j}_{\rm ex}$ are the external charge and current densities, respectively. In the system under consideration $\rho=\rho_1\delta(z+d/2)+\rho_2\delta(z-d/2)$ and $\mathbf{j}=\mathbf{j}_1\delta(z+d/2)+\mathbf{j}_2\delta(z-d/2)$,[37] so the charges and currents exist only in the 2D electron layers. There are no external currents and charges in the system: $\rho_{\rm ex}=\mathbf{j}_{\rm ex}=0$. In this case the potentials **A** and φ can be found from the homogeneous equations (3.2), (3.3). Using Fourier-transformation (2.7) and taking into account that $\mathbf{j}(\omega,\mathbf{k},z)=\mathbf{j}^{(1)}(\omega,\mathbf{k},-d/2)\delta(z+d/2)+\mathbf{j}^{(2)}(\omega,\mathbf{k},d/2)\delta(z-d/2)$ [with the upper indexes (1) and (2) indicating the first and the second layers], we obtain

$$\varphi(\omega,\mathbf{k},z)=\varphi_{\rm ex}(\omega,\mathbf{k},z)+\frac{2\pi}{p\varepsilon}\int_{-\infty}^{\infty}dz'\rho_{\rm in}(\omega,\mathbf{k},z')e^{-p|z-z'|}, \tag{3.5}$$

$$\mathbf{A}(\omega,\mathbf{k},z)=\mathbf{A}_{\rm ex}(\omega,\mathbf{k},z)+\frac{2\pi}{cp}\int_{-\infty}^{\infty}dz'\mathbf{j}_{\rm in}(\omega,\mathbf{k},z')e^{-p|z-z'|}, \tag{3.6}$$

where $p=\sqrt{k^2-(\omega^2/c^2)\varepsilon}$, Re$p>0$. It follows from Eqs. (3.5) and (3.6) that the electromagnetic waves exist in the system in the form of the surface waves localized in the vicinity of the DL2DES (see Fig. 1). In this case the component $A_z=0$, while the scalar potential can be found from the Lorentz gauge (2.14): $\mathbf{kA}=(\omega\varepsilon/c)\varphi$. Using Eqs. (2.7), (3.1), and (3.4), the current densities in the 2D electron layers of the DL2DES can be represented in the form

$$\mathbf{j}_\alpha^{(1)}(\omega,\mathbf{k})=i\frac{\omega}{c}\sigma_{\alpha\beta}^{(1)}(\omega,\mathbf{k})\left[A_\beta(\omega,\mathbf{k},-d/2)-\frac{c^2}{\varepsilon\omega^2}k_\beta k_\gamma A_\gamma(\omega,\mathbf{k},-d/2)\right], \tag{3.7}$$

$$\mathbf{j}_\alpha^{(2)}(\omega,\mathbf{k})=i\frac{\omega}{c}\sigma_{\alpha\beta}^{(2)}(\omega,\mathbf{k})\left[A_\beta(\omega,\mathbf{k},d/2)-\frac{c^2}{\varepsilon\omega^2}k_\beta k_\gamma A_\gamma(\omega,\mathbf{k},d/2)\right]. \tag{3.8}$$

The indices α, β, γ in Eqs. (3.7) and (3.8) take the values x and y. Using Eqs. (3.1)–(3.6), the vector potential of the electromagnetic fields in each layer of the DL2DES can be represented in the form

$$A_\alpha(\omega,\mathbf{k},-d/2)=\frac{2\pi}{cp}[j_\alpha^{(1)}(\omega,\mathbf{k})+j_\alpha^{(2)}(\omega,\mathbf{k})\exp(-pd)], \tag{3.9}$$

$$A_\alpha(\omega,\mathbf{k},d/2)=\frac{2\pi}{cp}[j_\alpha^{(1)}(\omega,\mathbf{k})\exp(-pd)+j_\alpha^{(2)}(\omega,\mathbf{k})]. \tag{3.10}$$

The dispersion relation is given by the determinant of the homogeneous system of equations (3.7)–(3.10),

$$[A^{(1)}\exp(pd)+B^{(1)}\exp(-pd)][A^{(2)}\exp(pd)+B^{(2)}\exp(-pd)]=D+C^{(1)}C^{(2)}, \tag{3.11}$$

where the following notations are introduced ($i=1,2$):

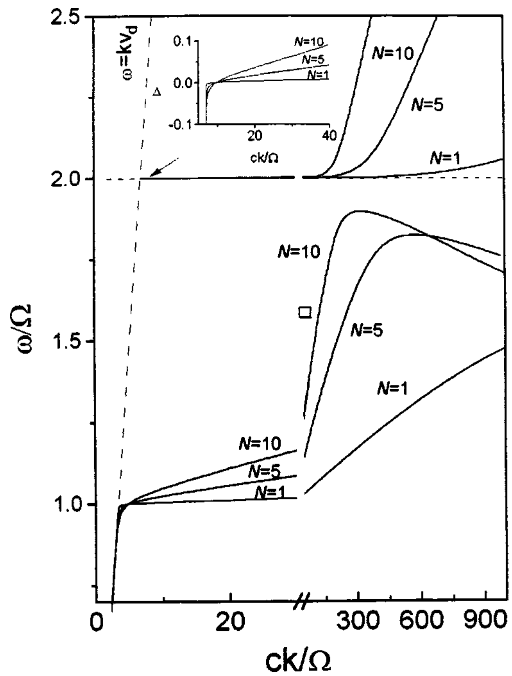

FIG. 3. The dispersion curves for the SP's for a one-layer 2DES calculated for various values of the Landau-level filling factor N ($N=1$, $N=5$, and $N=10$), $\Omega=10^{13}\ \mathrm{s}^{-1}$ (taken from Ref. 22).

$$A^{(i)}=B^{(i)}+F^{(i)}+\varepsilon,$$

$$B^{(i)}=\frac{2\pi}{c}\{[\sigma_{xx}^{(i)}]^2+[\sigma_{xy}^{(i)}]^2\},$$

$$F^{(i)}=i\,\frac{2\pi}{\omega p}\left(p^2-\frac{\omega^2}{c^2}\,\varepsilon\right)\sigma_{xx}^{(i)},$$

$$C^{(i)}=2B^{(i)}+F^{(i)},$$

$$D=\varepsilon\,\frac{2\pi}{c}\{[\sigma_{xx}^{(1)}-\sigma_{xx}^{(2)}]^2+[\sigma_{xy}^{(1)}-\sigma_{xy}^{(2)}]^2\}. \quad (3.12)$$

The conductivity tensor for ith ($i=1,2$) layer is determined by the expressions (2.14), (2.15),

$$\sigma_{\alpha\beta}^{(i)}(\omega,\mathbf{k})=\frac{2e^2}{h}\,\frac{\mathfrak{N}^{(i)}}{1+\gamma^{(i)2}}\left\{B_{\alpha\beta}^{(i)}-\frac{(kl)^2}{2\gamma^{(i)}}\left(1+\frac{\mathfrak{N}^{(i)}}{2}\right)C_{\alpha\beta}^{(i)}\right\}, \quad (3.13)$$

where $\mathfrak{N}^{(i)}$ is the Landau-level filling factor for the ith layer ($i=1,2$). We assume that each layer has its own value of the chemical potential, and its own value of the effective electron (hole) mass. Different values of the chemical potential for two layers can be realized, for example, by applying different gate voltages to the corresponding potential wells (see, e.g., Refs. 1 and 2).

Before considering the 2LDES, it is convenient first to discuss the dispersion relation of the SP in a high magnetic field for a one-layer 2DES.[22] Figure 3 (taken from Ref. 22) represents the dispersion curves of the SP propagating in the one-layer 2DES. The dispersion curves for the surface polaritons in the one-layer 2DES were calculated for various values of the Landau-level filling factor $\mathfrak{N}$ ($\mathfrak{N}=1$, $\mathfrak{N}=5$, and $\mathfrak{N}=10$). If the 2DES is realized using the heterostructure GaAs/Al$_x$Ga$_{1-x}$As, the effective electron mass $m=0.068m_0$ and $\varepsilon=12$. The y-axis shows the real part of frequency, and the x axis shows the value of the wave number. It is seen from Fig. 3 that the spectrum of the SP's is gapless at low frequencies ($\omega\ll\Omega$), and the SP's exist both in the low-frequency region $\omega<\Omega$, and in the high-frequency region $\omega>\Omega$. In the low-frequency region, far away from the CR, the phase velocity of the SP is close to the light velocity $v_d=c/\sqrt{\varepsilon}$ in the dielectric medium that surrounds the 2D electron layer. In the high-frequency region and in the vicinity of the principal CR ($\omega\sim\Omega$), the phase velocity of the SP's decreases drastically, and they are transformed into slow waves. In the frequency region $\Omega<\omega<2\Omega$, and under the condition $l^{-1}\gg k\gg(\omega/c)\sqrt{\varepsilon}$, one can neglect the retardation effect, and the spatial dispersion in the conductivity tensor is given by Eq. (2.11). In this case, the dispersion relation can be transformed into the form

$$\omega^2=\Omega^2+\frac{2\pi v_n k\Omega}{\varepsilon}, \quad (3.14)$$

where $v_n=(2e^2/h)\mathfrak{N}$. It is easy to see that when $\Omega\gg(v_nk/\varepsilon)(\mathfrak{N}\sim 1)$, the dispersion law of the SP is linear ($\omega-\Omega\sim k$), while in the opposite case $\Omega\ll(v_nk/\varepsilon)$ (or when $\mathfrak{N}\gg 1$), the dispersion relation is of a square-root type ($\omega\sim\sqrt{k}$).

Near the CR ($\omega\sim\Omega$) one cannot neglect the retardation effect, and the dispersion law of the SP has the form

$$\omega=\Omega+\Omega\,\frac{v_n}{c}\left\{\frac{\pi\Omega}{cp_1}\left(\frac{p_1^2c^2}{\varepsilon\Omega^2}-1\right)+\frac{2\pi^2v_n}{\varepsilon c}\right\}-i\nu. \quad (3.15)$$

Here $p_1=\sqrt{k^2-(\Omega^2/c^2)\varepsilon}$. The value of the relative deceleration of the SP is determined by the fine-structure constant α. The group velocity, $\mathbf{v}_g=(\partial\omega/\partial\mathbf{k})$, of the SP undergoes fundamental steps in the vicinity of the CR:

$$\frac{v_g}{v_d}=\frac{2\sqrt{2}\alpha\mathfrak{N}}{\sqrt{\varepsilon}}. \quad (3.16)$$

Thus, the deceleration of the wave near the CR is significant, and the reason for the quantization of the group velocity is the quantization of the Hall conductivity, i.e., the system possesses a fundamental parameter (which has the dimension of velocity)—the conductance quantum $2e^2/h$. At the point of the CR the character of the conductivity changes, and the imaginary part of the conductivity becomes large. This leads to the occurrence of the slow waves (the slow SP's).[22] With further increase of the frequency ω, near the CR subharmonic ($\omega\sim 2\Omega$), the spatial dispersion effects of the conductivity (2.11) become noticeable; the group velocity changes its sign and takes negative values. In this region the SP's show anomalous (negative) dispersion.

The SP spectrum near the CR subharmonic ($\omega\sim 2\Omega$) has the form

$$\omega=2\Omega-\Omega\,\frac{b}{d}\left(\frac{kl}{2}\right)^2\left(1+\frac{\mathfrak{N}}{2}\right)-i\nu. \quad (3.17)$$

Here

$$b=\frac{v_n}{c}\left(\frac{4\pi}{3}\right)\left(\frac{\Omega}{cp}\right)\left(1-\frac{p_2^2c^2}{4\varepsilon\Omega}\right), \tag{3.18}$$

$d=1+2b$, and $p_2=\sqrt{k^2-(4\Omega^2/c^2)\varepsilon}$. At $\omega>2\Omega$, the SP propagates through the system at a velocity close to that of the SP far away from the CR subharmonic (see Fig. 3). It follows from Eqs. (3.17), (3.18) that the dispersion curve of the SP is closely pinned to the line of the CR subharmonic ($\omega=2\Omega$). The dispersion curve of the SP near the CR subharmonic has a characteristic scale set by the small parameter $\Delta=\hbar\Omega/mc^2\ll1$. This dispersion curve (see the insert in Fig. 3) of the SP starts near the fundamental mode of the light line ($\omega=kv_d$), then it branches upwards (the number of branches is equal to the Landau-level filling factor $\mathfrak{N}$), and the group velocity is quantized in the same way as near the principal CR ($\omega=\Omega$). But in the case of the CR subharmonic, the group velocity is very low $v_g\sim v_d(\hbar\Omega/mc^2)$ in the region of the wave numbers where the dispersion curve is closely pinned to the line $\omega=2\Omega$. The dispersion curve of the SP approaches the line $\omega=2\Omega$ for $k<\varepsilon\Omega/v_n$. At $k\sim\varepsilon\Omega/v_n$ the dispersion curve separates from the line $\omega=2\Omega$ (see Fig. 3). The relative attenuating rate of the SP is of the order ν/ω and is small for the samples with a high electron mobility.

In the case of two identical layers in the DL2DES (nn-type or pp-type), the dispersion relations are given by the expressions,

$$2\left(\frac{2\pi}{c}\right)^2[\sigma_{xx}^2+\sigma_{xy}^2][ch(pd)\pm1]+i\,\frac{2\pi\sigma_{xx}}{\omega p}\left(p^2-\frac{\omega^2}{c^2}\,\varepsilon\right)\times[\exp(pd)\pm1]+\varepsilon\,\exp(pd)=0. \tag{3.19}$$

In the limiting case when the interlayer distance $d\to0$, the dispersion relation takes the form equivalent to a one-layer system,[22]

$$\left(\frac{2\pi}{c}\right)^2\{[\sigma_{xx}^{(1)}+\sigma_{xx}^{(2)}]^2+[\sigma_{xy}^{(1)}+\sigma_{xy}^{(2)}]^2\}+i\,\frac{2\pi[\sigma_{xx}^{(1)}+\sigma_{xx}^{(2)}]}{\omega p}\left(p^2-\frac{\omega^2}{c^2}\,\varepsilon\right)+\varepsilon=0, \tag{3.20}$$

where the longitudinal components ($\sigma_{xx}^{\rm ef}=\sigma_{xx}^{(1)}+\sigma_{xx}^{(2)}$) and the Hall components ($\sigma_{xy}^{\rm ef}=\sigma_{xy}^{(1)}+\sigma_{xy}^{(2)}$) of the effective conductivity tensor should be introduced.

A. *nn*-type double-layer 2DES

Let us consider the nn-type DL2DES in the case when the Landau-level filling factor is the same for each layer ($\mathfrak{N}=\mathfrak{N}_1=\mathfrak{N}_2$). The dispersion curves determined by the dispersion relation (3.19) for the high mobility electrons ($\nu\to0$) in a DL2DES are shown in Fig. 4.

Generally, the dispersion curves are of the same type as the dispersion curves for the one-layer system. Near the principal CR the phase velocity is slowed down, and the group velocity undergoes the fundamental steps [see Fig. 3 and Eqs. (3.14)–(3.16) for different values of the Landau-level filling factor $\mathfrak{N}$]. In Fig. 4 the dotted line describes the dispersion curve for a one-layer system and for $\mathfrak{N}=1$. For the

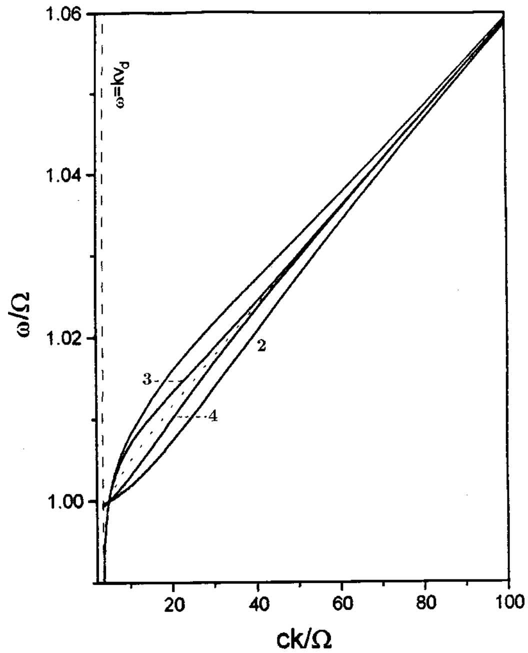

FIG. 4. The dispersion curves for the SP for a double-layer 2DES (nn-type). The Landau level filling factors: ($N_1=N_2=1$). The interior split curves (1 and 2): $d\Omega/c=0.1$. The exterior split curves (3 and 4): $d\Omega/c=0.05$. The dotted line is the dispersion curve for a one-layer 2DES. The dashed line is the light line $\omega=kv_d$, where $v_d=c/\varepsilon^{1/2}$.

DL2DES each dispersion curve (for different $\mathfrak{N}$) is split into two modes. The splitting of the SP dispersion curves is significant in the long-wave region, $kd<1$. A lower curve (the mode indicated by the "$-$" sign in Eq. (3.22)] has the endpoints of the spectrum $p=0$ that are located at the light line $\omega=kv_d$. These endpoints (for the curves 2 and 4 in Fig. 4) are determined from the equation $\omega=\Omega/[1+2\alpha\mathfrak{N}(d\Omega/c)]$. The group velocity v_g of the SP near the principal CR ($\omega\sim\Omega$), is

$$\frac{v_g}{v_d}=2\alpha\mathfrak{N}\sqrt{\frac{2}{\varepsilon}}\,[1\pm\exp(-\sqrt{\varepsilon}d\Omega/c)],\quad v_d=c/\sqrt{\varepsilon}. \tag{3.21}$$

When $\sqrt{\varepsilon}d\Omega/c\ll1$, the group velocity is given by the expression,

$$\frac{v_g}{v_d}=\begin{cases}4\alpha\mathfrak{N}\sqrt{\dfrac{2}{\varepsilon}}, & \text{``+'' mode},\\ 2\sqrt{2}\alpha\mathfrak{N}d\Omega/c, & \text{``$-$'' mode}.\end{cases} \tag{3.22}$$

So, in the DL2DES two slow SP's propagate. The "$-$" mode (lower line 2 or 4 in Fig. 4) describes the strongly correlated collective electromagnetic excitations (SP's). The group velocity of the "$-$" mode is smaller than for the "+" mode, and smaller than the group velocity for the one-layer system[22] [see Fig. 3, Eq. (3.14), Eq. (3.16)]. The splitting of the dispersion curves is vanishingly small in the short-wave region (see Fig. 4).

Figures 5(a) and 5(b) show the dispersion curves ($at\,\nu\ll\Omega$) for the DL2DES, when the Landau-level filling factors

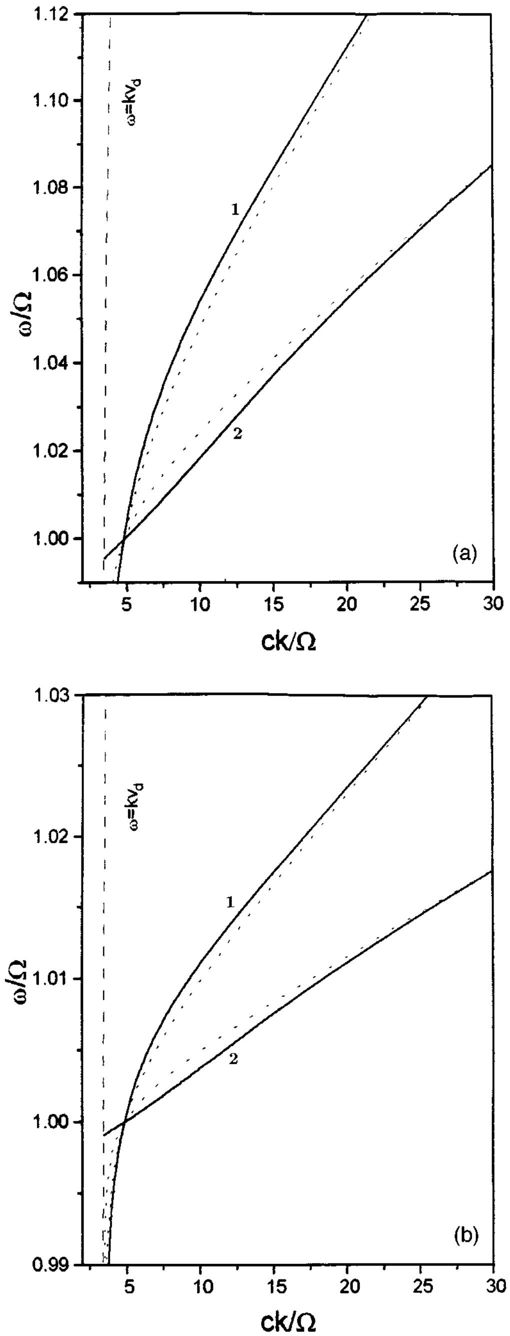

FIG. 5. The dispersion curves for the SP of a DL2DES (nn-type) for different values of the Landau-level filling factor N (solid lines 1 and 2). The dotted lines are the corresponding dispersion curves for the one-layer 2DES: (a) curve 1, $N_1=10$; curve 2, $N_2=5$; $d\Omega/c=0.1$; (b) curve 1, $N_1=2$; curve 2, $N_2=1$; $d\Omega/c=0.1$; $\Omega=10^{13}\ \mathrm{s}^{-1}$.

are different for different layers $(\mathfrak{N}_1 \neq \mathfrak{N}_2)$. Near the principal CR the group velocity is described by the formula

$$\frac{v_g}{v_d}=2\alpha\sqrt{\frac{2}{\varepsilon}}\left[\frac{\mathfrak{N}_1+\mathfrak{N}_2}{2}\right.$$
$$\left.\pm\sqrt{\left(\frac{\mathfrak{N}_1-\mathfrak{N}_2}{2}\right)^2+\mathfrak{N}_1\mathfrak{N}_2\ \exp(-2\sqrt{\varepsilon}d\Omega/c)}\right]. \tag{3.23}$$

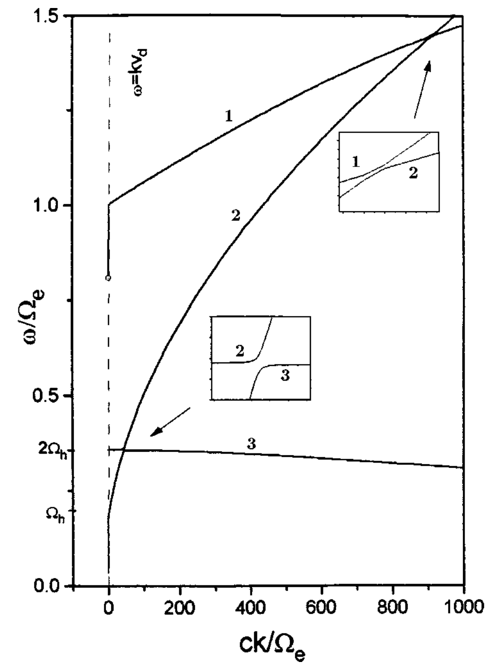

FIG. 6. The dispersion curves for the SP of a DL2DES (np-type), $N_e=5$ and $N_h=10$; $d\Omega_e/c=0.1$. The curve 1 corresponds to the electron CR; the curves 2 and 3 correspond to the hole CR's at the principal hole CR $(\omega=\Omega_h)$, and at its subharmonic $(\omega=2\Omega_h)$; $\Omega_e=10^{13}\ \mathrm{s}^{-1}$.

Figure 5(a) demonstrates the dispersion curves for the case, when the Landau-level filling factors are $\mathfrak{N}_1=5$ and $\mathfrak{N}_2=10$ [solid lines 1 and 2 in Fig. 5(a)]. The dotted lines in Fig. 5(a) demonstrate the corresponding dispersion curves for a one-layer 2DES. Figure 5(b) shows the dispersion curves for $\mathfrak{N}_1=1$ and $\mathfrak{N}_2=2$. Both cases represented in Figs. 5(a) and 5(b) demonstrate that the lower spectral line possesses the endpoints on the light line $\omega=kv_d$. It is easy to see from Figs. 4, 5(a), 5(b) that one of the two SP modes is slower than the SP in a one-layer 2DES with the Landau-level filling factor $\mathfrak{N}=\min[\mathfrak{N}_1,\mathfrak{N}_2]$. The other SP mode is faster than the SP for a one-layer 2DES with $\mathfrak{N}=\max[\mathfrak{N}_1,\mathfrak{N}_2]$. The slower mode has the endpoint in the spectrum $p=0$. With decreasing of the interlayer distance d (Fig. 1), one mode slows down, and the other mode is accelerated [see Eqs. (3.21), (3.22), and (3.23)]. Near the principal CR $(\omega\sim\Omega)$ the accelerated mode approaches a one-layer 2DES dispersion curve with an effective value of the Landau-level filling factor $\mathfrak{N}=\mathfrak{N}_1+\mathfrak{N}_2$. In the case, when the DL2DES is of the pp-type, the picture for the dispersion curves is the same as is shown in Figs. 4, 5(a), 5(b).

B. np-type of double-layer 2DES

Figure 6 shows the dispersion curves for the np-type DL2DES. Near the subharmonic of the holes CR the spectral curves in the long-wave limit represent two interacting modes (curves 2 and 3 in Fig. 6). The first mode (curve 2 in Fig. 6) is generated near the hole subharmonics $(\omega\sim 2\Omega_h)$, another mode (curve 3 in Fig. 6) is generated near the principal (hole) CR $(\omega\sim\Omega_h)$. The dispersion curve 3 in Fig. 6 possesses the anomalous (negative) dispersion at short wavelengths. In the short-wavelength region the dispersion curve

1 is generated by the principal (electron) CR ($\omega \sim \Omega_e$) that is strongly interacting with the SP mode (curve 2 in Fig. 6) which is generated near the subharmonic (hole) CR. The mode 1 occurs at the endpoint of the spectral curve. The endpoint of the mode 1 is located on the light line $\omega = kv_d$, and its coordinate is

$$\omega = \Omega_e \left[\frac{m_e}{m_h} \frac{m_e \mathfrak{N}_1 + m_h \mathfrak{N}_2}{m_h \mathfrak{N}_1 + m_e \mathfrak{N}_2 + 4\alpha \mathfrak{N}_1 \mathfrak{N}_2 m_e d \Omega_e / c} \right]^{1/2}. \tag{3.24}$$

Thus, near the principal (hole) CR ($\omega \sim \Omega_h$), and near the subharmonic of (hole) CR ($\omega \sim 2\Omega_h$) one mode of the SP exists, which is the same as in the one-layer (hole) 2DES. Near the subharmonic (hole) CR ($\omega \sim 2\Omega_h$) the SP mode possesses the negative (anomalous) dispersion. The second SP mode occurs near the principal (electron) CR ($\omega \sim \Omega_e$), and its exhibits the endpoint of the spectrum ($p=0$). In the short-wave region both SP modes exhibit a mutual resonance interaction, where they interchange the energy, and their localization regions vary. The resonance interaction of two modes (curves 1 and 2 in Fig. 6) of the SP takes place near the point (ω_0, k_0):

$$\omega_0 = \Omega_e \left[\frac{m_e}{m_h} \frac{\mathfrak{N}_h m_h - \mathfrak{N}_e m_e}{\mathfrak{N}_h m_e - \mathfrak{N}_e m_e} \right]^{1/2}, \tag{3.25}$$

$$k_0 = \frac{\varepsilon \Omega_e}{2\alpha c m_h} \frac{m_h^2 - m_e^2}{\mathfrak{N}_h m_e - \mathfrak{N}_e m_h}. \tag{3.26}$$

The insets in Fig. 6 demonstrate the fine structure of the dispersion curves near the points where the modes strongly interact. In the system of coordinates near the point (3.25), (3.26) the dispersion curves are described by a simple equation

$$a_1 (\Delta\omega)^2 - a_2 (\Delta k)^2 = \exp(-2\omega_0 d/c), \tag{3.27}$$

where

$$a_1 = \frac{\omega_0^2 \varepsilon^2 m_h}{\alpha^2 \mathfrak{N}_1 \mathfrak{N}_2 k_0^2 c^2 \Omega_e^2 m_e}, \quad \alpha_2 = k_0^{-2} \left[1 + \frac{\mathfrak{N}_h m_e}{\mathfrak{N}_e m_h} + \frac{\mathfrak{N}_e m_h}{\mathfrak{N}_h m_e} \right],$$

with $\Delta\omega = \omega - \omega_0$, and $\Delta k = k - k_0$.

In a one-layer 2DES another type of SP exists (see Ref. 22), which appears near the CR ($\omega \sim \Omega$). This SP is a dissipative-type wave. As was mentioned above, the surface waves exist when Re$p>0$. At the same time, when the relaxation frequency $\nu \neq 0$, the frequency ω is complex. A straightforward analysis shows that the ASP mode is practically nondissipative, and its existence is determined by the threshold condition,

$$\frac{\nu}{\Omega} > 2\alpha \frac{\mathfrak{N}}{\sqrt{\epsilon}}. \tag{3.28}$$

Thus, the dissipation can influence the SP dispersion properties and can lead to new interesting features. When ν exceeds a critical value [see Eq. (3.28)], the SP dispersion curve splits into two branches (see Fig. 4 in Ref. 22). One of those curves practically coincides with the light line ($\omega' = ck/\sqrt{\epsilon}$), and has the endpoint of the spectrum Re$p=0$. At this point the SP field is delocalized. As is seen from Eq. (3.31) (see, also, Ref. 22), the threshold condition for the ASP occurrence in a high magnetic field is determined by the fine-structure constant α, and by the quantized value of the Landau-level filling factor. Thus, the threshold condition (3.31) for the ASP existence in a high magnetic field is determined by the discrete value $\mathfrak{N}$ due to the Hall quantization. The spatial dispersion of the conductivity (2.14) of the 2DES in a high magnetic field does not significantly influences either the ASP threshold condition or the ASP spectrum and damping. Note that the experimental observation of such an ASP specifies the relaxation frequency ν with an accuracy up to the fine-structure constant α.

In a DL2DES (see Fig. 1) the ASP also exists. The dispersion relation for the ASP is

$$\omega = \omega' + i\omega'', \tag{3.29}$$

$$\omega' = \Omega_e \left[1 \pm \frac{2\alpha\mathfrak{N}}{\sqrt{\varepsilon}} \exp(\omega'' d\sqrt{\varepsilon}/c) \sin(\omega' d\sqrt{\varepsilon}/c) \right],$$

$$\omega'' = -\nu + \frac{2\alpha\mathfrak{N}\Omega_e}{\sqrt{\varepsilon}} [1 \pm \exp(\omega'' d/\sqrt{\varepsilon}/c) \sin(\omega' d\sqrt{\varepsilon}/c)]. \tag{3.30}$$

Equations (3.29), (3.30) can be solved iteratively, using the small parameter $2\alpha\mathfrak{N}/\sqrt{\varepsilon} \ll 1$. In this case,

$$\omega' = 1 \pm \frac{2\alpha\mathfrak{N}}{\sqrt{\varepsilon}} \exp(-\nu d\sqrt{\varepsilon}/c) \sin(\Omega_e d\sqrt{\varepsilon}/c), \tag{3.31}$$

$$\omega'' = -\nu + \frac{2\alpha\mathfrak{N}\Omega_e}{\sqrt{\varepsilon}} [1 \pm \exp(-\nu d\sqrt{\varepsilon}/c) \cos(\Omega_e d\sqrt{\varepsilon}/c)]. \tag{3.32}$$

The threshold condition for the ASP occurrence in the DL2DES has the form ($\omega'' < 0$),

$$\nu > \frac{2\alpha\mathfrak{N}\Omega_e}{\sqrt{\varepsilon}} [1 \pm \exp(-\nu d\sqrt{\varepsilon}/c) \cos(\Omega_e d\sqrt{\varepsilon}/c)]. \tag{3.33}$$

This condition looks like Eq. (3.31) but it reflects different values of the threshold for each split ASP mode [the signs "$\pm$" in (3.36)]. The threshold (3.36) possesses geometrical oscillations as a function of the magnetic field and the interlayer distance d.

Figures 7(a)–7(d) demonstrate the dispersion and the damping of the SP and the ASP, when the threshold conditions (3.36) are met. Figure 7(a) ($\mathfrak{N}_1 = \mathfrak{N}_2 = 1$, $\nu/\Omega_e = 0.1$, $d\Omega_e/c = 0.1$) shows that at such values of the relaxation frequency ν the split ASP in the DL2DES of nn-type appears (dispersion curves 1 and 2, and the corresponding dampings, the curves 4 and 5). The ASP has the endpoint of the spectrum defined by the condition Re$p=0$ (dispersion curve 3). The damping of the corresponding SP increases sharply (curve 7 transforms into curve 4) near the principal CR, where the SP drastically decelerates. The ASP exists from the left side of the light line $\omega = kv_d$, and represents the delocalization wave because it is only weakly pinned to

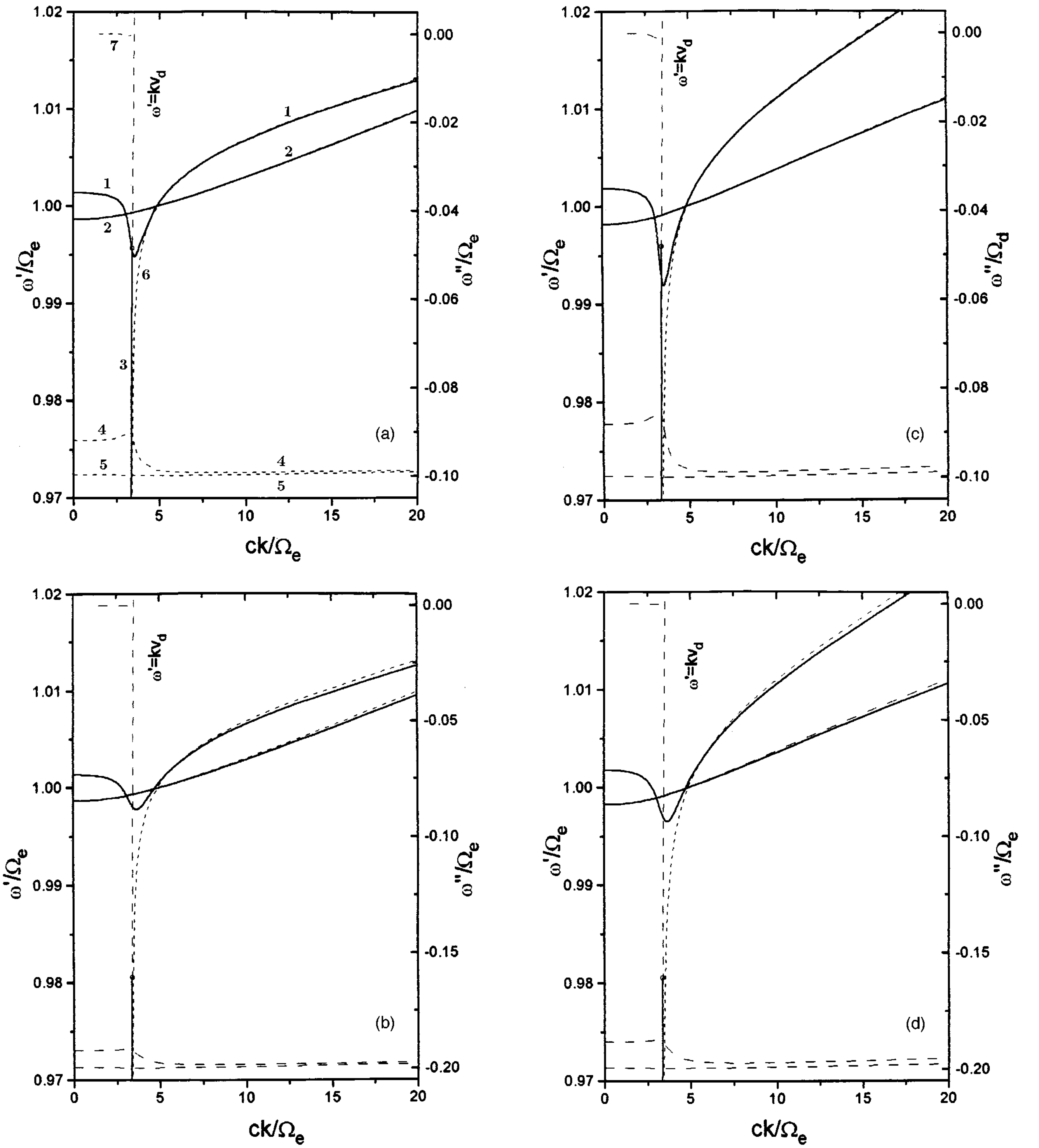

FIG. 7. Dispersion curves (ω')—solid lines 1, 2, and 3, and the corresponding dampings (ω'')—dashed lines 4 and 5 of the SP's, and ASP's in a DL2DES. The dashed line 6 is the dispersion curve of the SP when the collision frequency ν is below the threshold given by Eq. (3.31); (a) $N_1=N_2=1$, $\nu/\Omega_e=0.1$, $d\Omega_e/c=0.1$; (b) $N_1=N_2=1$, $\nu/\Omega_e=0.2$, $d\Omega_e/c=0.1$; (c) $N_1=1$, $N_2=2$, $\nu/\Omega a_e=0.1$, $d\Omega_e/c=0.1$; (d) $N_1=1$, $N_2=2$, $\nu/\Omega_e=0.2$, $d\Omega_e/c=0.1$.

the DL2DES. The SP is a surface wave, which is strongly pinned to the DL2DES far from the principal mode (the light line) $\omega=kv_d$. In the DL2DES the dispersion curves 1 and 2 split near the CR, and the faster mode (1) has a minimum near the light line. When the relaxation frequency increases [Fig. 7(b)] the endpoint of the main mode 3 ($\omega=kv_d$) moves down from the principal CR. Figure 7(c) ($\mathfrak{N}_1=1$, $\mathfrak{N}_2=2$, $\nu/\Omega_e=0.1$, $d\Omega_e/c=0.1$) shows that for different values of the Landau-level filling factor the splitting of the dispersion curves 1 and 2 increases, and the minimum for the faster mode 1 becomes deeper and sharper. Figure 7(d) ($\mathfrak{N}_1=1$, $\mathfrak{N}_2=2$, $\nu/\Omega_e=0.2$, $d\Omega_e/c=0.1$) is similar to Fig. 7(c), but with increased values of the relaxation frequency ν. In this case, the endpoint moves down from the CR, and the minimum of the faster mode (curve 1) becomes smoother. The curves 4, 5 for the damping of the SP (the right-hand side of the light line) in the series of pictures shown in Fig. 7 are qualitatively similar. The damping of the SP becomes strong near the CR, where the SP is drastically decelerated, and is of order ν/Ω. When the relaxation frequency ν increases, the endpoint of the principal mode (curve 3 in Fig. 7) moves down, and this mode becomes significantly separated from the SP and the ASP modes.

IV. CONCLUSION

In conclusion, we have calculated explicitly the spectrum of collective excitations, damping and polarization in a double-layer 2DES in a high magnetic field—the slow surface polaritons, when the effects of quantization are essential. We used the Wigner distribution function formalism for the calculation of the spatial and time dispersion of the conductivity tensor for each layer in the double layer 2DES in a high magnetic field. Near the CR the phase velocity of a SP drastically slows down, and the group velocity of a SP undergoes fundamental steps, whose magnitude is determined by the fine-structure constant $\alpha = e^2/\hbar c$. Thus, in a high magnetic field under the IQHE condition, the dispersion characteristics of the SP in a one-layer 2DES and in a double-layer 2DES are also quantized. Also, due to the spatial dispersion of the conductivity, the group velocity of the SP becomes negative (anomalous) near the CR subharmonics. For the nn-type DL2DES each dispersion curve splits, and strongly correlated collective electromagnetic excitations (SP) propagate in the system. The group velocity of one of the split SP modes is smaller than that for the one-layer 2DES. For the np-type DL2DES the branches of the SP strongly interact in the long-wave region [near the subharmonic (hole) CR], and in the short-wave region, due to interaction between the subharmonic (hole) CR mode and the principal (electron) CR mode. When the relaxation frequency exceeds a critical threshold condition, in the one-layer 2DES and in the double-layer 2DES, the ASP's occur—a new mode of surface electromagnetic oscillations. As a consequence, the dispersion curves of the SP and of the ASP change significantly—spectrum endpoints and mode confluence appear. In a double-layer 2DES the threshold condition for the ASP has an oscillating form due to the coherence effects between split SP modes.

Note that the phase velocity of the SP has a remarkably small value near the CR. Thus, the double-layer 2D electron systems represent an effectively decelerating systems under the IQHE condition. This fact could be used for various applications in microelectronics and for the contactless measurements of the quantum Hall effect in new materials (e.g., organic conductors). Also, it can be used for excitation of surface electromagnetic waves by a beam of charged particles which passes near 2D electron layers, and for the efficient conversion of the beam energy into the wave energy.

In recent experiments[21] (see also the excellent review by Pinczuk[39] and references herein) the collective excitations in 2DES under the quantum Hall regime were observed, using the resonant inelastic light scattering method.[39,40] The dispersion curves of the collective excitations observed in Refs. 21 and 39 for one-layer 2DES qualitatively coincide with the results represented in Fig. 3, when the Landau-level filling factor $\mathfrak{N} = 1$. In Refs. 21, 39 the authors give the explanation of the observed dispersive collective excitations as a manifestation of the electron-electron interaction, including the time-dependent Hartree-Fock approximation,[41,42] single-mode approximation,[43] and numerical studies.[44] In Refs. 41–44 the spectrum of magnetoplasmon excitations was calculated. These excitations are the bulk type modes (not the surface excitations), and of a longitudinal type. As it was shown in Ref. 22 and in our present paper, in the 2DES and in the DL2DES the geometric factor plays a significant role, and the excitations are of the surface type—SP and ASP (and not only the bulk eigenmodes, as those considered in Refs. 41–44). The polarization and the spectral properties of these excitations are generally more complicated and informative. Namely, the spectrum, damping and polarization of the SP and ASP considered in Ref. 22 for 2DES and in this paper for the DL2DES depend significantly on the geometric factor. Measurements of polarization of the SP and ASP, and the spectral behavior as a function of the Landau-level filling factor are of significant interest.

ACKNOWLEDGMENTS

One of us (I.E.A.) is grateful to B. Altshuler and to Yu. Lu for fruitful discussions, and to the Theoretical Division and the Center for Nonlinear Studies of the Los Alamos National Laboratory for hospitality during the completion of this work. This research was partly supported by the INTAS Grant No. 94-3862, and by Ukrainian Committee of Science and Technology (Project No. 2.3/19 ‘‘Metal’’). Work at Los Alamos was supported by the Defense Advanced Research Projects Agency.

[1] Y. W. Suen, L. W. Engel, M. B. Santos, M. Shayegan, and D. C. Tsui, Phys. Rev. Lett. **68**, 1379 (1992); J. P. Eisenstein, G. S. Boebinger, L. N. Pfeiffer, K. W. West, and S. He, *ibid.* **68**, 1383 (1992).

[2] S. Q. Murphy, J. P. Eisenstein, G. S. Boebinger, L. N. Pfeiffer, and K. W. West, Phys. Rev. Lett. **72**, 728 (1994).

[3] K. Moon, H. Mori, Kun Yang, S. M. Girvin, A. H. MacDonald, L. Zheng, D. Yoshioka, and Shou-Cheng Zhang, Phys. Rev. B **51**, 5138 (1995); Kun Yang, K. Moon, L. Zheng, A. H. MacDonald, S. M. Girvin, D. Yoshioka, and Shou-Cheng Zhang, Phys. Rev. Lett. **72**, 732 (1994).

[4] A. H. MacDonald and Shou-Cheng Zhang, Phys. Rev. B **49**, 17 208 (1994).

[5] X. G. Wen and A. Zee, Phys. Rev. Lett. **69**, 1811 (1992); Phys. Rev. B **47**, 2265 (1993).

[6] Z. F. Ezawa and A. Iwazaki, Int. J. Mod. Phys. B **6**, 3205 (1992); Phys. Rev. B **47**, 7295 (1993); **48**, 15 189 (1993).

[7] A. H. MacDonald, P. M. Platzman, and G. S. Boebinger, Phys. Rev. Lett. **65**, 775 (1990).

[8] L. Brey, Phys. Rev. Lett. **65**, 903 (1990); H. A. Fertig, Phys. Rev. B **40**, 1087 (1989); O. Narikiyo and D. Yoshioka, J. Phys. Soc. Jpn. **62**, 1612 (1993).

[9] R. Gote, L. Breg, and A. H. MacDonald, Phys. Rev. B **46**, 10 239 (1992); X. M. Chen and J. J. Quinn, *ibid.* **45**, 11 054 (1992); J. Smoliner, E. Gornik, and G. Weinmann, Appl. Phys. Lett. **52**, 2136 (1988); J. Smoliner, W. Demmerle, G. Berthold, E. Gornik, G. Weinmann, and W. Schlapp, Phys. Rev. Lett. **63**, 2116 (1989); Phys. Rev. B **40**, 3049 (1991); J. P. Eisentein, L. N. Pfeiffer, and K. W. West, Appl. Phys. Lett. **58**, 1497 (1991); J. P. Eisentein *et al.*, Phys. Rev. Lett. **68**, 1383 (1992).

[10] B. I. Galperin, Helv. Phys. Acta **56**, 75 (1983); T. Chakraborty and P. Pietiläinen, Phys. Rev. Lett. **59**, 2784 (1987); E. H. Rezayi and F. D. M. Haldane, Bull. Am. Phys. Soc. **32**, 892 (1987); Song He, S. Das.Sarma, and X. C. Xie, Phys. Rev. B **47**, 4394 (1993); D. Yoshioka, A. H. MacDonald, and S. M. Girvin, *ibid.* **39**, 1932 (1989); for a brief review on the FQHE in the double-layer systems see A. H. MacDonald, Surf. Sci. B **47**, 229 (1990); **47**, 1 (1990).

[11] K. Moon, Phys. Rev. Lett. **78**, 3741 (1997).

[12] E. S. Sorensen and A. H. MacDonald, Phys. Rev. B **54**, 10 675 (1996).

[13] A. S. Plaut, A. Pinczuk, B. S. Dennis, J. P. Eisenstein, L. N. Pfeiffer, and K. W. West, Surf. Sci. **361/362**, 158 (1996).

[14] N. Turner, J. T. Nichols, E. H. Linfield, K. M. Brown, G. A. C. Jones, and D. A. Ritchie, Phys. Rev. B **54**, 10 614 (1996).

[15] D. L. Mills and E. Burstein, Rep. Prog. Phys. **37**, 817 (1974); E. Burstein, A. Hartstein, J. Schoenwald, A. A. Maradudin, D. L. Mills, and R. F. Wallis, in *Interfaces in Polaritons*, edited by E. Burstein and F. de Martini (Pergamon, New York, 1974), p. 89; A. A. Maradudin, in *Surface Polaritons. Electromagnetic Waves at Surfaces and Interfaces*, edited by V. M. Agranovich and D. L. Mills (North-Holland, Amsterdam, 1982), p. 405; M. G. Cottam and A. A. Maradudin, in *Surface Excitations*, edited by V. M. Agranovich, and R. Loudon (Elsevier, Amsterdam, 1984); I. M. Kaganova, Phys. Rev. B **51**, 5333 (1995).

[16] F. G. Elmzughi, N. C. Constantinou, and D. R. Tilley, J. Phys.: Condens. Matter **7**, 315 (1995).

[17] C. S. Ting, S. C. Ying, and J. J. Quinn, Phys. Rev. Lett. **37**, 215 (1976); Phys. Rev. B **16**, 5394 (1977); N. J. M. Horing and M. Yildiz, Phys. Lett. **44A**, 386 (1973); Ann. Phys. (N.Y.) **97**, 216 (1976); K. M. Chiu and J. J. Quinn, Phys. Rev. B **9**, 4724 (1974); Yu. A. Kosevich, A. M. Kosevich, and J. C. Granada, Phys. Lett. A **127**, 52 (1988).

[18] G. Gumbs and G. R. Aizin, Phys. Rev. B **51**, 7074 (1995); G. R. Aizin and G. Gumbs, *ibid.* **52**, 1980 (1995).

[19] E. Vasiliadou, G. Muller, D. Heitman, D. Weiss, K. von Klitzing, H. Nickel, W. Schlapp, and R. Losch, Phys. Rev. B **48**, 17 145 (1993).

[20] V. L. Tal'yanskii, Pis'ma Zh. Eksp. Teor. Fiz. **43**, 96 (1986) [JETP Lett. **43**, 127 (1986)]; L. Vendler and M. I. Kaganov, *ibid.* **44**, 345 (1986) [**44**, 445 (1986)]; N. N. Beletskii, E. A. Gasan, and V. M. Yakovenko, *ibid.* **45**, 589 (1987) [**45**, 751 (1987)]; A. Tselis, G. G. De la Cruz, and J. J. Quinn, Solid State Commun. **47**, 43 (1983); A. Tselis and J. J. Quinn, Phys. Rev. B **29**, 2021 (1986); Wu Fi-Wei, P. Hawrylak, G. Eliasson, and J. J. Quinn, *ibid.* **33**, 7091 (1986); I. D. Vagner and D. Bergman, *ibid.* **35**, 9856 (1987); M. Wassermeier, J. Oshinowo, J. P. Kotthaus, A. H. MacDonald, C. T. Foxon, and J. J. Harris, *ibid.* **41**, 10 287 (1990); I. E. Aronov, I. V. Krive, S. A. Naftulin, and G. Wendin, Mod. Phys. Lett. B **8**, 1135 (1994).

[21] L. L. Sohn, A. Pinczuk, B. S. Dennis, L. N. Pfeiffer, and K. W. West, Solid State Commun. **93**, 897 (1995).

[22] I. E. Aronov and N. N. Beletskii, J. Phys.: Condens. Matter **8**, 4919 (1996).

[23] E. Wigner, Phys. Rev. **40**, 749 (1932).

[24] A. I. Akhiezer and S. V. Peletminskii, *Methods of Statistical Physics* (Pergamon, Oxford, New York, 1981).

[25] E. N. Bogacheck, I. O. Kulik, and R. I. Shekhter, Solid State Commun. **56**, 999 (1985).

[26] D. K. Ferry and H. L. Grubin, Solid State Phys. **49**, 283 (1995)]; N. C. Kluksdahl, A. M. Kriman, D. K. Ferry, and C. Ringhofer, Phys. Rev. B **39**, 7720 (1989); J.-R. Zhou and D. K. Ferry, IEEE Trans. Electron Devices **39**, 473 (1992).

[27] W. R. Frensley, Phys. Rev. B **36**, 1570 (1987).

[28] A. A. Abrikosov, *Fundamentals of the Theory of Metals* (North-Holland, Amsterdam, 1988).

[29] I. M. Lifshits, M. Ya. Azbel, and M. I. Kaganov, *Electron Theory of Metals* (Colsultans Bureau, New York, 1973).

[30] V. F. Gandmacher and Y. B. Levinson, in *Modern Problems in Condensed Matter Sciences*, edited by V. M. Agranovich and A. A. Maradudin (North-Holland, New York, 1987), Vol. 19.

[31] E. M. Lifshitz and L. P. Pitaevskii, *Physical Kinetics* (Pergamon, New York, 1983).

[32] I. E. Aronov and I. V. Krive, Low Temp. Phys. **20**, 259 (1994).

[33] E. A. Kaner, O. I. Lyubimov, I. E. Aronov, and R. I. Shekhter, Sov. Phys. Semicond. **4**, 43 (1970).

[34] A. M. Chang and D. C. Tsui, Solid State Commun. **56**, 153 (1985); H. L. Störmer *et al.*, *ibid.* **84**, 95 (1992); T. Rötger *et al.*, Phys. Rev. Lett. **62**, 90 (1989); S. H. Simon and B. I. Halperin, *ibid.* **73**, 3278 (1994).

[35] See, e.g., J. P. Cheng and B. D. McCombe, Phys. Rev. Lett. **64**, 3171 (1990).

[36] See, e.g., J. D. Jackson, *Classical Electrodynamics* (Wiley, New York, 1962).

[37] A. L. Fetter, Ann. Phys. (N.Y.) **81**, 367 (1973).

[38] The principal mode of the SP ($\omega = kv_d$) and the slow SP and ASP are determined by interactions of various natures (different symmetries) in the 2QES. In the present case we do not encounter a violation of the noncrossing theorem [see, L. D. Landau and E. M. Lifshits, *Quantum Mechanics* (Pergamon, New York, 1977)].

[39] A. Pinczuk, in ''*Perspectives in Quantum Hall Effect*,'' edited by S. Das Sarma and A. Pinchuk (Wiley, New York, 1977), p. 307.

[40] E. Burstein, A. Pinchuk, and S. Buchner, in *Physics of Semiconductors, 1978*, edited by B. L. Wilson, IOP Conf. Proc. No. 43 (Institute of Physics and Physical Society, London, 1979), p. 1231.

[41] C. Kallin and B. I. Halperin, Phys. Rev. B **30**, 5655 (1985).

[42] A. H. MacDonald, J. Phys. C **18**, 1003 (1985).

[43] A. H. MacDonald, H. C. A. Oji, and S. M. Girvin, Phys. Rev. Lett. **55**, 2208 (1985); S. M. Girvin, A. H. MacDonald, and P. M. Platzman, *ibid.* **54**, 581 (1985).

[44] F. D. M. Haldane and E. H. Rezayi, Phys. Rev. Lett. **54**, 237 (1985).